

Experimental and computational studies on savonius wind rotor: A comprehensive review

Yogi Manash Reddy N.^{1,*}, Swarna Kumari A.²

¹ Assistant Professor, Department of Mechanical Engineering, Maturi Venkata Subba Rao (MVSR) Engineering College, Hyderabad, Telangana, India.

² Professor, Department of Mechanical Engineering, JNTUK, Kakinada, Andhra Pradesh, India.

Abstract:

It is axiomatic that the savonius wind turbine suits perfectly as a stand-alone power system for built environments with its merits: simple design, low noise, low-cost maintenance, no yawing mechanism needed, and self-starts at low wind speeds. However, it suffers low efficiency owing to various non-optimal design parameters. Additionally, the negative torque developed at the returning blade is the predominant influencing factor for the low performance of the savonius rotor. This work summarizes the savonius rotor and its performance-influencing parameters, including its geometric and aerodynamic properties, emphasizing several wind augmentation techniques employed. Few researchers happened to review the savonius rotors in the last decade. This paper provides a clear understanding of the test data used to experiment on savonius rotors. Thus, this work aims to collect and review various experimental and computational investigations on savonius rotors and present noteworthy findings for future researchers' benefit.

Keywords: Vertical Axis Wind Turbine (VAWT), Savonius rotor, Wind augmentation technique, Wind tunnel blockage effect, Tip Speed Ratio, Aspect Ratio, Overlap Ratio, lift & drag forces.

Contents

1. Introduction
2. Savonius rotor - Performance parameters
 - 2.1 Tip speed ratio
 - 2.2 Bucket overlap ratio
 - 2.3 Aspect ratio
 - 2.4 Blade profiles and rotor shapes
 - 2.5 Number of buckets and rotor stages
 - 2.6 End plates
 - 2.7 Reynolds number
 - 2.8 Lift and Drag forces
3. Wind tunnel blockage effects
4. WADs and their effect in performance enhancement of S-rotor
5. Experimental studies on S-rotor
6. Computational studies on S-rotor
7. Summary and discussion on S-rotor
8. Conclusion and Recommendation

1. Introduction:

The rise in human population worldwide has dramatically increased energy demand, eventually increasing fossil fuels' usage. The upsurge usage of conventional energy sources geared climate change rapidly, bringing in extreme weather conditions, such as floods, droughts, and storms in the past few decades [1].

Researchers worldwide are developing and improving renewable energy conversion methods to help tackle the rising energy demand. Notably, efficient and affordable stand-alone renewable energy power systems may restrict the dependence on fossil fuels. Wind energy has enormous potential among all the renewable energy

sources to be a primary source of generating electricity with zero-emission [2]. Wind energy converters are classified according to their aerodynamic function: lift or drag force created by wind stream on turbine blades and, secondly, with respect to their axis of rotation i.e. horizontal axis wind turbines (HAWTs) for which the rotor axis of rotation is horizontal to the ground surface and vertical axis wind turbines (VAWTs) for which the rotor axis of rotation is vertical to the ground surface [3].

VAWTs remain appropriate for turbulent winds and are beneficial for built environments and wind shadow areas with simple design, low noise, and a smaller footprint. Moreover, researchers found that wind farms perform better by swapping HAWTs with VAWTs [4]. However, VAWTs suffer to self-start at low wind speeds and are less efficient than HAWTs [5]–[7]. Furthermore, VAWTs are classified into lift-type: Darrieus rotor and H-rotor, and drag-type: Sistan rotor and Savonius rotor. The drag-type rotors have a better self-starting ability [8]–[10] than lift-type rotors but suffer low efficiency [8]. Though the Sistan windmills are the earliest wind rotors ever used [11]–[14], the Savonius rotor has grabbed all the attention with its high starting ability at lower wind speeds.

Savonius rotor (often called S-rotor due to its cross-section similar to the alphabet 'S') is a drag-type VAWT developed in the late 1920s by a Finnish engineer, Sigurd Johannes Savonius [15]. Researchers and the general public have widely accepted the S-rotor with its merits; simple design, ability to generate power at low wind speeds, omnidirectional, low noise, low maintenance, and aptness for confined spaces. However, S-rotor suffers low performance [8]. Henceforth, several research enthusiasts all over the world worked to improve the performance of the savonius rotor by pursuing various studies related to design configurations [5], [16], blade shapes [9], the number of cups or blades [10], and the number of steps or stages [17], [18]. Nevertheless, the low performance of the S-rotor is due to the negative torque established by the opposing wind force at the convex side of the returning blade, resulting in a drip of net positive torque [19], [20]. Addressing this problem, investigators developed various wind augmentation devices (WADs), viz curtain design, ducts, deflector plate, concentrators, and windshields [20], [21]. These WADs significantly reduced the negative torque and also enhanced the performance of the S-rotor. Many scholars have attempted to review the S-rotor and its performance criteria in the last decade. However, no single review paper discusses the standard S-rotor testing conditions. This study will evaluate various experimental and computational research on performance affecting parameters and wind augmentation methods of a Savonius rotor, focusing on test data, including wind tunnel blockage effects, and recommend test conditions to be adopted to experiment on S-rotor.

2. Savonius rotor - Performance parameters

A conventional savonius rotor [15], [22] comprises two cup-shaped blades attached with overlap to a rotating shaft as illustrated in Fig. 1. When the wind blows through the system and interacts with the two blades (convex and concave), two forces (lift and drag) are imparted to those two surfaces. Hence, the essential principle is the difference in the drag observed between the convex and concave parts of the blades when rotor blades revolve around a vertical shaft. Though it is a drag-type rotor, a slight lift force also backs to power the rotor [23]. The most significant benefit of an S-rotor remains its capability to cut-in at low wind speeds compared to Lift type VAWTs [24], which makes it a commercially feasible off-grid power generation system for urban applications.

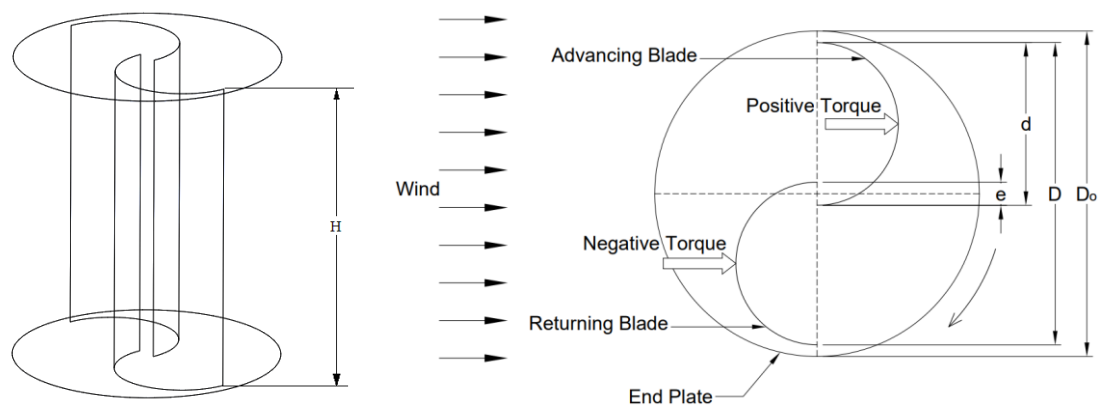


Fig. 1 Savonius rotor (H-Height of the blade, D-Diameter of the rotor, D_0 -Diameter of the end plate, d-Blade diameter, e-Blade overlap distance)

The performance of an S-rotor depends on its torque coefficient (C_T) and power coefficient (C_P). C_T is the ratio of the turbine torque (T_t) to the torque available (T_a). Similarly, C_P is the ratio of turbine power (P_t) to the wind's theoretical power (P_a). P_a is the ratio of kinetic energy in the wind to time. Wind power is directly proportional to wind velocity's cube (the third power) [25]. As a result, increasing the wind velocity that reaches a wind turbine can enhance its power output significantly.

$$P_a = \frac{1}{2} \rho A v^3 \quad (1)$$

$$C_T = \frac{F \times r}{\frac{\rho a v^2 R}{2}} \quad (2)$$

$$C_P = \frac{T_t \times \omega}{\frac{\rho A v^3}{2}} \quad (3)$$

The wind striking the S-rotor at a certain velocity primes the advancing blade with positive torque and retards the returning blade with a negative torque, as shown in Fig. 1. Moreover, torque on the concave blade (advancing/positive torque) of the S-rotor is high compared to the torque on the convex blade (returning/negative torque) because of the dissimilar resistance coefficients of the blade surfaces [26], [27], making the S-rotor rotate in the path of the positive torque.

Savonius stated that the maximum efficiency obtained from S-rotor is 31% [22]. However, several researchers worldwide worked on optimizing various geometric and aerodynamic properties viz Tip Speed Ratio (TSR), Bucket overlap ratio (OR), Rotor Aspect ratio (AR), Rotor shapes (blade profiles), number of blades and stages, End-plates, Reynolds number (range of wind speeds), lift force and drag force to increase the efficiency of the S-rotor. Moreover, the performance of an S-rotor increases considerably by involving various stators (WADs).

2.1 Tip speed ratio

The S-rotor Tip Speed Ratio (TSR or λ) is a dimensionless factor defined as the ratio of the speed of the S-rotor tip to the air stream wind velocity [28], which depends on the blade airfoil contour used and the number of blades. The coefficient of torque decreases with the increase in the tip speed ratio. Therefore, the S-rotor power coefficient is proved to be ideal at TSR=0.7-1.0 [29].

$$\lambda = \frac{\omega R}{V} \quad (4)$$

2.2 Bucket overlap ratio

The S-rotor's bucket overlap ratio (OR= e/d) is an essential geometric parameter to increase the performance of the rotor. With the increase in overlapping distance (e) between the buckets, the air stream that passes through the overlap increases and acts on the returning bucket's concave side, eventually increasing the static torque coefficient (C_{TS}). However, an OR of 0.20 to 0.50 is optimum for maximum performance[30].

2.3 Aspect ratio

The aspect ratio of the S-rotor system is the ratio of Height (H) to the diameter (D). As the AR of the S-rotor increases, the air stream flowing on the rotor increases, thereby increasing the torque. Nevertheless, the moment of inertia decreases. Therefore, for higher wind speed zones, a higher AR is desirable to improve the performance of the S-rotor. Rotors with ARs ranging between 1.0-2.0 are proved to be performing better [31]. A comparison of several aspect ratios at varying wind speeds is studied by researchers [32]. It has been discovered that as the aspect ratio rises from 0.60 to 0.80, the rotor's performance rises too. Beyond this point, the performance begins to decrease.

2.4 Blade profiles and rotor shapes

Various blade shapes have been invented in the last few decades to increase the efficiency of the S-rotor. The first is a Savonius-designed semicircular profile [15], [22] (Fig. 2(a)). Later Bach rotor was developed by Back G. in 1931 with a better performance capability [33], [34] (Fig. 2(b)).

Numerous works were done on bach type to study and enhance the performance of bach type rotor [23], [35]–[40]. A swinging rotor was developed by Aldos [41] (Fig. 2(c)) to increase the performance by decreasing the negative torque on the returning blade. Benesh developed a rotor on his name [42], [43] (Fig. 2(d)). However, it is less efficient than bach type rotor [39]. Reupke and Probert decreased the negative torque on the returning blade by introducing a slatted blade rotor [44] (Fig. 2(e)). Numerous studies [35][45]–[50] explored a twisted

blade rotor (Fig. 2(f)), which is said to be the best rotor for solving the negative torque issue on the returning blade while also improving the starting torque. A fish ridge type rotor [51] (Fig. 2(g)), Elliptical rotor [37], Slotted blade rotor [52], [53] (Fig. 2(h)), and more are investigated and found to be better performing compared to conventional savonius rotor giving a clear picture that there is absolute scope to increase the rotor performance by working on the blade profile.

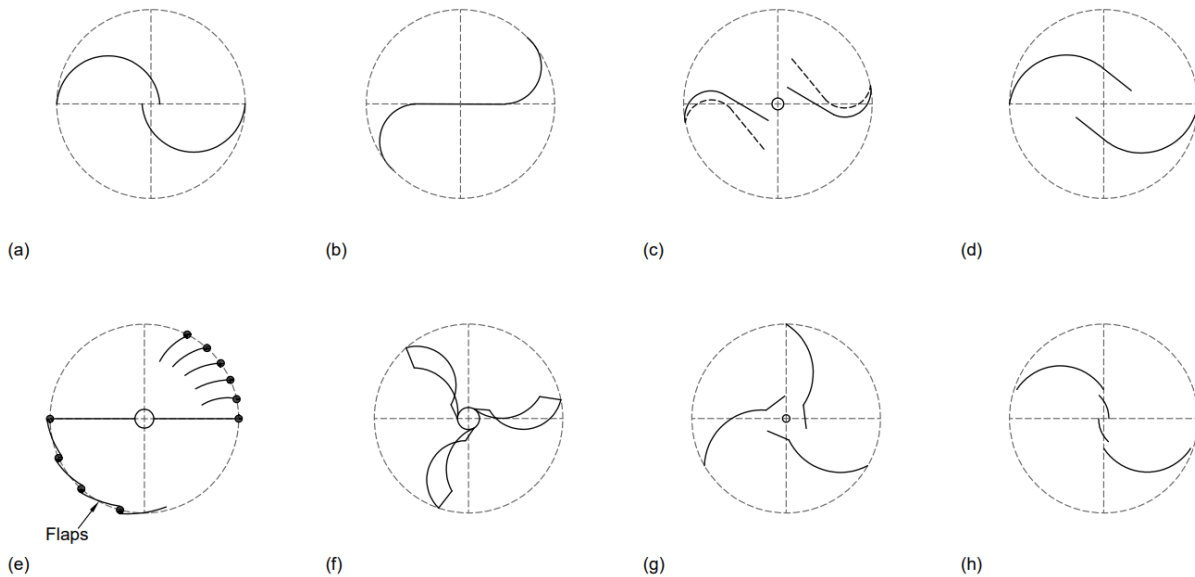


Fig. 2 Various savonius blade shapes and profiles (a) Semicircular, (b) Bach, (c) Swinging, (d) Benesh, (e) Slatted, (f) Twisted, (g) Fish-ridged, and (h) Slotted

2.5 Number of buckets and rotor stages

The efficiency of S-rotors depends on the number of buckets [54]. In general, an S-rotor consists of 2 to 4 buckets. A two-blade rotor outperformed a three-blade rotor. [55]. On the other hand, a three-cup S-rotor has better starting capability compared to a two-cup rotor. However, vortices formation behind the blade reduces the rotor's performance. The S-rotor staging can solve the challenge of improving starting torque without forming vortices. Staging has an impact on the aerodynamic behavior of S-rotors [18]. A two stage S-rotor (Fig. 3) exhibited a higher power coefficient compared to single-step and three-step rotors. [16].

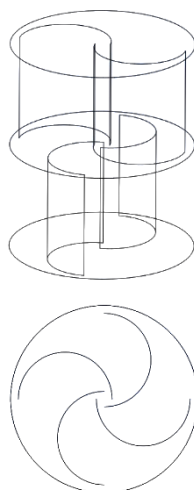


Fig. 3 Two stage S-rotor (4 blades in total)

2.6 End plates

The end plate is a component attached at the top end and bottom end of the S-rotor (Fig. 1), used to stop the wind stream from escaping through the rotor concave side, thereby maintaining the pressure difference between

rotor blades to enhance its performance significantly. The optimal end plate diameter (D_o) is 1.1 times the S-rotor diameter (D)[8].

2.7 Reynolds number

The performance of the S-rotor dramatically depends on the aerodynamic parameter, Reynolds number (Re). The efficiency of the S-rotor increases with the increase of Re [56].

2.8 Lift and Drag forces

The S-rotor is not a perfect drag type device, despite the fact that drag is the primary driving force. The rotor behaves like a thin body at a reduced blade angle, and a modest lift power adds responsiveness to the net force, according to reports [57].

S-rotor operates mainly on drag (C_D), nonetheless it also experiences less lift force (C_L). It is evident from research that at low to moderate TSRs, the torque produced by the S-rotor is not solely due to drag characteristics. However, at high TSRs, relative effect of C_L diminishes, and C_D takes over as the primary driver of rotor rotation.[58], [59].

3 Wind tunnel blockage effects

One vital factor to pay attention to in experimental investigations using wind tunnels is the blockage effect. Wind tunnel blockage effects arise when a wind stream flows through the wind rotor, becoming an obstacle blocking the air stream. As a result, wind tunnel test findings are inaccurate without blockage rectification.

The blockage effect depends on the blockage ratio (BR), which is the ratio of the projected area of the S-rotor to the wind tunnel cross-sectional area. However, a less than 10% BR showed a negligible blockage effect [60]. Moreover, an S-rotor model tested in different wind tunnels (having dissimilar BR s) exhibited dissimilar results owing to the change in the blockage effect.

4 WADs and their effect in performance enhancement of S-rotor

Researchers noted the negative torque created at the returning blade side of an S-rotor as a significant issue. Wind Augmentation increases the S-rotor system's performance by increasing incoming wind velocity while minimizing the negative torque on the returning blade.

With the use of windshields, negative torque is decreased, allowing the improvement in S-rotor's performance. These shields (flat or circular) are generally positioned in forward-facing of the returning cup to minimize the wind pressure on it. The effect of adding flat shields and end plates to a rotor was investigated by Alexander & Holownia [61] (Fig. 4(a)), and the performance was found to be greatly improved.

The deflecting plate has been employed as a power boost to accelerate the wind striking on the rotor surface and lower airstream resistance on the S-rotor (returning blade) rotating opposite direction of the air stream. The circular end plate is regarded to be the best option. The power has been enhanced by around 24% by using a deflecting plate before the rotor [62]. The rotor harnessed around 20% more power with the ideally pitched deflector situated at its optimal location [63] (Fig. 4(b)). The use of a valve-aided rotor [64] (Fig. 4(c)) reduces negative torque on the returning blade, increasing the power coefficient.

A novel curtain arrangement (Fig. 4(d)) at the rotor front is developed [65] to enhance the efficiency of the S-rotor by avoiding the negative torque that opposes S-rotor movement. There was a 16 % gain in performance when comparing curtain to curtainless rotors. Venting (Fig. 4(e)) is reported to be more effective to decrease the thrust load on returning blade [66]. While venting improves power generation only somewhat, capping considerably boosts it.

The rotor's performance was improved by 32.3 % over the free stream condition by using an oriented and concentrated jet [19] (Fig. 4(f)). The guide vane minimizes negative torque and increases exerted positive torque by effectively and smoothly guiding inflowing air. The rotor with the highest power coefficient was nearly 40% larger than the rotor without guiding blades [67].

A stator vane is designed [68] (Fig. 4(g)) in such a way that the vanes should simultaneously channel the flow to the advancing blade while also limiting the flow that interacts with the returning blade. A conveyor-deflector curtain system [69] (Fig. 4(h)) with two aerodynamic attachments is designed to partially enclose the S-rotor. The conveyor, which sits alongside the moving blade, is designed to direct incoming wind toward the rotor. The deflector, which is situated close to the returning blade, reduces the dynamic pressure applied to it.

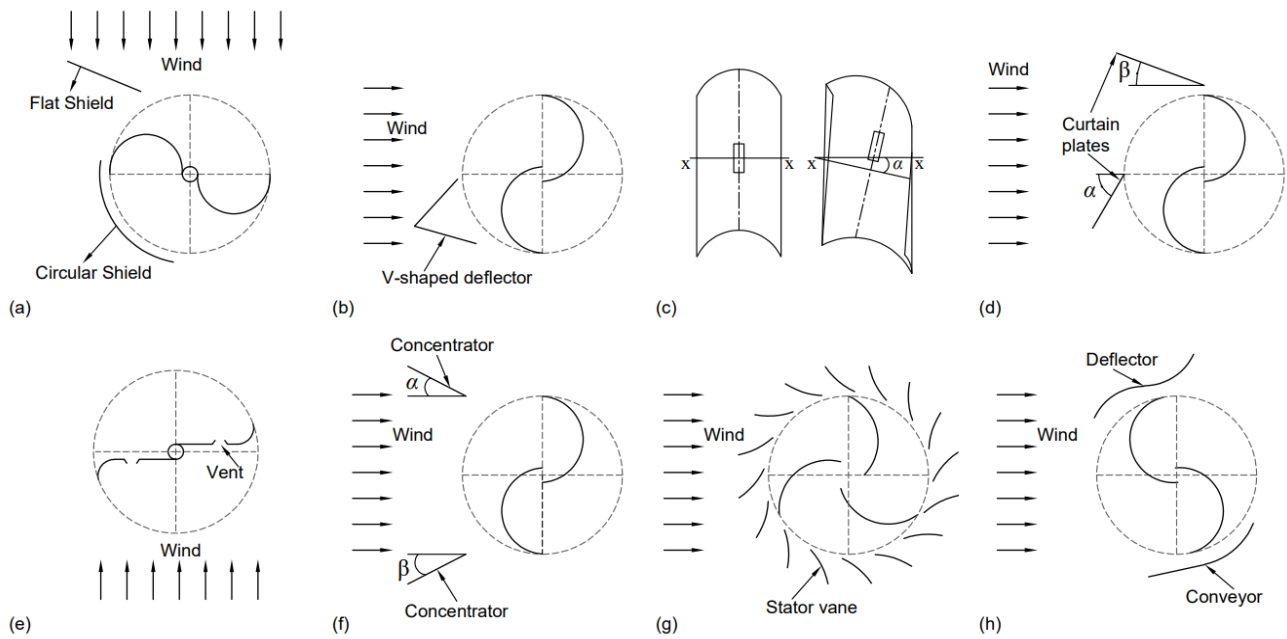


Fig. 4 Various wind augmentation devices for S-rotor (a) Wind shields, (b) V-shaped deflector, (c) Valve, (d) Curtain plates, (e) Vent, (f) Concentrator, (g) Stator vane, and (h) Conveyor-deflector

5 Experimental studies on S-rotor

To experiment with savonius rotor, a low-speed wind tunnel, static and dynamic torque sensors, wind anemometers are often used by researchers. Unfortunately, wind tunnel tests every so often suffers from blockage effects. The wind tunnel blockage ratio, BR (projected area of the rotor to the wind tunnel cross-sectional area), is the decisive factor in amending the blockage effects in wind tunnel tests. It is to observe that the standard practice is to operate a low-speed wind tunnel with $BR < 10$ as the blockage effects will be minimal. However, if $BR > 10$, a few correlations were given by researchers to correct the blockage effect. S-rotor is to be placed 2m from wind tunnel exit to offer uniform air flow [16], [64],[70]. Table 1 summarizes various experimental studies on S-rotors, providing brief test conditions and wind tunnel blockage correction (if any).

Table 1 Few experimental studies on S-rotor with brief test parameters

Investigator(s)	AR	Overlap distance/OR	Wind velocity	TSR (λ)	No. of blades and cross section	Wind tunnel Blockage correction	Observation
Modi & Fernando [71]	0.77	0	17.9 m/s	0.71 & 0.79	2	blockage 17%	At a TSR = 0.79, the highest C_p of 0.32 was recorded.
Fujisawa & Gotoh [72]	1	OR=1.5	6 m/s	0.9	2 (Semicircular)	not considered	At TSR = 0.9, the C_p is at its highest.
Kamoji et al. [35]	1,0.88,0.93,1.2,1,1	0,0,0,0,0.1,0.16	4 m/s to 14 m/s	0.65 - 0.71	2 (6 types of helical Savonius rotor)	39%, effect of blockage ratio is negligible on C_p , C_T and C_{ST} for rotors in an open jet wind tunnel	The helical S-rotor has a lower TSR for maximum C_p than the standard S-rotor.

Investigator(s)	AR	Overlap distance/OR	Wind velocity	TSR (λ)	No. of blades and cross section	Wind tunnel Blockage correction	Observation
Damak et al. [49]	1.57	0	6 m/s to 11.1 m/s	0.4-0.45	2 (helical Savonius rotor)	not mentioned	The C_T increases nearly linearly as the TSR decreases.
Nasef et al. [73]	1	0.15	6 m/s	0.2 to 1.4	2 (Semicircular)	25%	As the TSR grows, the C_T of the rotor decreases.
Banerjee et al. [74]	1.1	20% of blade chord	6.2 m/s	0.2 to 1.2	2 (elliptical & Semicircular)	Blockage correction factor, $f=f(V,N,F)$, Where V is wind speed, F is load, and N is speed of the rotor [60]	TSR = 0.80 results in the best performance for both turbines.
Jeon et al. [75]	2	0	6 m/s to 12 m/s	0.49 - 0.57	2 (4 types of helical Savonius rotor)	varies from 3% to 8.3%	The C_T decreases as the TSR rises.
Lee et al. [45]	1.33	0.167	8 m/s & 10 m/s	0.4-0.8	2 (Semicircular)	BR=0.092	At a TSR = 0.6, the maximum C_P is observed.
Ricci et al. [76]	2.6	18 mm	7.3 m/s to 12.7 m/s	0.2 to 1.2	2 (helical)	Blockage factor $\epsilon=A/4S$, where A is rotor swept area and S is wind tunnel test section area	At TSR around 0.60, the highest performance for all turbines is observed.
Mojola [77]	1.53	OR=0.125 to 0.875	not mentioned	0.4 to 1.6	2 (Semicircular)	not mentioned	When the OR is around 0.25, the C_P is at its highest.
Jian et al. [78]	1.088	0,0.167 & 0.333	4 m/s to 10 m/s	0.2 to 1.6	2 (Semicircular)	0.068 -single stage & 0.136-double stage	At an OR of 0.167, a high C_P was reported. Although OR has an effect on the C_P and C_T of two-stage rotors, it is not significant.
Kumbruss et al. [79]	2.16 (2-stage), 1.08	0,0.16, 0.32	4 m/s to 10 m/s	0-1.4	2,3 (Semicircular)	Double-stage:13.75%, single-stage: 6.75%	A higher OR on improving the starting characteristics is significant.

Investigator(s)	AR	Overlap distance/OR	Wind velocity	TSR (λ)	No. of blades and cross section	Wind tunnel Blockage correction	Observation
Kamaji et al. [30]	1	0.1,0.15,0.2,0.23,0.5,0.7	120000 to 200000	0.4-1.4	2 (Semicircular)	20%,28% and 35%	The C_{ST} increases as the OR increases from 0.1 to 0.5. The C_{ST} declines when the OR is increased to 0.7, implying that an OR of 0.5 gives the largest C_{ST} .
Alexander & Holownia [61]	1.2 to 4.8	12.5 mm (Negative Overlap)	6 m/s to 9 m/s	0.72	2, 3 & 4 (Semicircular)	Velocity corrections of more than 50% for S/C values greater than 0.32	The highest efficiency of 0.243 is attained at a high AR (4.8) and ideal design. Whether shielded or not, three and four-bladed rotors were less efficient than two-bladed rotors. A three-bladed rotor's starting characteristics proved superior to a two-bladed rotor.
Modi et al. [80]	0.91	38 mm	17.9 m/s	0.6 to 1.6	2 (4 configurations)	Blockage correction avoided	For a given wind velocity, an increase in gap size causes the maximum output to occur at a higher shaft speed.
Plourd et al. [66]	1.18	No overlap	4.53 m/s to 11.81 m/s	-	2 (solid, venting & venting-capping)	0.23 (corrected wind speeds can be obtained by multiplying with 1.23)	Venting improves power generation only slightly, capping significantly enhances it.
Hayashi et al. [81]	1.25	OR=0.2	6 m/s to 18 m/s	0 to 1.5	2 (Semicircular)	3.50%	The C_{ST} of both rotors are unaffected by the Reynolds number.
Damak et al. [82]	0.7	0	4.9 m/s to 8.75 m/s	0.15 to 1.25	2 (Helical Bach rotor)	26 %, blockage effect is insignificant.	The Helical Bach rotor (HBR) offered a more significant C_P and a better C_{ST} than the helical rotor.

6. Computational studies on S-rotor:

It is obvious to say that the results obtained from the experimental investigations are more accurate than computational. However, Computational Fluid Dynamics (CFD) can help reduce experimentation time and costs. Researchers worldwide have used various CFD techniques such as Finite Volume Method (FVM), Finite Difference Method (FDM), and Finite Element Method (FEM) to discretize the flow governing equations around S-rotor. Nevertheless, Finite Volume-based methodologies are proven to be more accurate in predicting the flow behavior of the S-rotor and have been used widely in the last decade. The basic procedure behind computational studies is represented in Fig. 5.

Table 2 Step by step procedure of the computational study

Pre-processing	Specification of computational domain, modelling, grid generation, meshing, defining flow properties and specifying boundary conditions
Solver	Discretization solvers like FDM, FVM & FEM are used in approximating the unknown variables and substituting them in flow governing equations to obtain solution
Post-processing	Visualisation of results using vector, contour, surface plots etc.

A turbulent flow field exists around an S-rotor. Thus, when choosing a numerical approach, turbulence characteristics must be considered. However, each turbulence model has its own set of advantages and disadvantages. A brief observation of various turbulence models is given in Table 3.

Table 3 Turbulence models employed to test savonius rotor

Turbulence Model	Observation
Spalart-Allmaras (SA) [83]	SA turbulence model is a one-equation model. Poor results reported in near-wall behaviour of an S-rotor [84]
Standard k-ϵ	In comparison to the Spalart-Allmaras turbulence model, standard k- ϵ predicted better [9]
Renormalization (RNG) k-ϵ	Improved accuracy observed in the case of swirling streams around the S-rotor [85], [86] 3-D simulations detected to be more precise compared to 2-D [87]
Realizable k-ϵ	Studies have shown that realizable k- ϵ models forecast better than regular k- ϵ and SA models.
Standard k-ω	Smaller C_T and C_P values are forecasted by the standard k- ω model. This model is vastly applied to boundary-layer flows with varying pressure gradients.
shear stress transport (SST) k-ω	Derived by combining the features of k- ϵ and k- ω models, The 2-D simulations overpredicted the experimental results. [88].

The following section (Table 4) provides an overview of numerous computational studies on Savonius wind rotors for the last ten years, including the turbulence models used.

Table 4 Few computational studies on S-rotor with brief test parameters

Investigator(s)	AR	Overlap distance/OR	Wind velocity	TSR (λ) Operating range	No. of blades and cross section	CFD Methodology	Observation
Zhenzhou Zhao et al. [89]	2	1,3,5,6,7	10 m/s	0.3 to 1.0	2 (helical)	2D, standard k- ϵ	The C_{ST} for helical Savonius rotors evaluated in this work are positive at all rotor angles. However, there are several rotor angles where the C_{ST} is negative for a conventional S-rotor.
Altan B. D. et al. [27]	1	26 mm	7 m/s	not mentioned	2 (Semicircular)	2D, standard k- ϵ	The performance of the s-rotor with a curtain is superior to that of the rotor without a curtain.

Investigator(s)	AR	Overlap distance/OR	Wind velocity	TSR (λ) Operating range	No. of blades and cross section	CFD Methodology	Observation
Mohamed M. H. et al. [24]	-	-	10 m/s	0.3 to 1.4	2	2D, Realizable $k-\epsilon$	Self-starting capability is achieved by the optimal design.
Kianifar A. et al. [90]	-	0, 3.2, 3.8, 6.4, and 7.2 cm	8 to 14 m/s	0.2 to 1.7	2	2D, standard $k-\epsilon$	The maximum value of the power coefficient appears at the range of $\lambda = 0.8$ to 1
Plourde B.D. et al. [91]	0.98	No overlap	8 m/s	0.52	2	3D, SST $k-\omega$	Capping and venting reduced thrust stress on the tower and boosted power production.
Sukanta Roy et al. [92]	1	0 to 0.30	5.57 m/s to 10.44 m/s	-	2	2D, Realizable $k-\epsilon$	The static torque increases when the OR increases, primarily due to increasing pressure on the concave side of the turbine returning blade.
Jaohindy P. et al. [93]	1.1	0.2	7 m/s	0 to 1.6	2	3D, RANS $k-\epsilon$ and $k-\omega$ SST	The validation findings reveal that both models have difficulty estimating the high rotor angular velocity.
Banerjee A. et al. [74]	-	20% of Chord length = 0.2d	6.2 m/s	0.2 to 1.2	2 (elliptical)	2D, SST $k-\omega$	When elliptical blades are used instead of semicircular blades, performance is boosted to 10.7%.
Kacprzak K. et al. [94]	0.77	0 to 0.30	9 m/s	0.4 to 1.2	2	2D, SST $k-\epsilon$	The maximum value of the C_p remained constant in the range of ORs up to 0.15. The highest investigated OR (0.30) shows a significant decrease in the C_p
Baz A.M. et al. [95]	-	0.2	9 m/s	0.4 to 1.4	2	2D, Realizable $k-\epsilon$	The C_p of the optimized two and three rotor arrangements is higher than that of the single rotor arrangement.
Mao Z. et al. [96]	-	-	7 m/s	0.6 to 1.4	2	2D, RNG $k-\epsilon$	The C_p is 8.37% higher than that of conventional S-rotor.
Driss Z. et al. [97]	3	-	3 m/s	-	2 (bucket arc angles varied)	2D, standard $k-\epsilon$	The bucket design (changing bucket angle) directly affects the local features.
Tian W. et al. [98]	-	-	7 m/s	0.4 to 1.2	2	2D, RNG $k-\epsilon$	The rotor with $n = 1$ blade fullness has the highest coefficient of power, 0.2573, 10.98% more than a standard S-rotor.

Investigator(s)	AR	Overlap distance/OR	Wind velocity	TSR (λ) Operating range	No. of blades and cross section	CFD Methodology	Observation
Shaheen M. et al. [99]	1	0.15	7 m/s	-	2	2D, SST $k-\omega$	a three-turbine cluster observed to be performing better.
El-Askary W. A. et al. [100]	1	0.15	6 m/s	0.3 to 2.2	2	2D, SST $k-\omega$	The new design's performance with the curved channel shape is the finest.
Driss Z. et al. [101]	3	-	3 m/s	-	2	2D, standard $k-\epsilon$	The incidence angle has a proportional effect on the local characteristics of the rotor.
Alom, N. et al. [102]	0.7	20% of Chord length = 0.2d	6.2 m/s	0.8	2 (elliptical)	2D & 3D SST $k-\omega$	When comparing the semi-circular and elliptical profiles, the elliptical profile outperforms the semi-circular one by 18.18 percent.
Jae-Hoon Lee et al. [45]	1.33	0.167	8 to 9.2 m/s	0.4 to 0.8	2 (helical)	3D, RNG $K-\epsilon$	At a twist angle of 45° , the maximum C_p estimates nearly 0.13.
Frikha S. et al. [18]	1.15	0.034	3 m/s	-	2 (one to five-stage varied Semicircular)	3D, modified $k-\epsilon$	the number of stages affects the aerodynamic behavior of the S-rotor
Moazam Sheikh H. et al. [103]	0.49	0 to 0.2	5 m/s	0.4 to 1.2	2	2D, SST $k-\omega$	The turbulence model was validated against experimental results and found to be accurate enough.
Alom, N. et al. [104]	-	0 to 0.30	6.2 m/s	0.2 to 1.2	2 (elliptical)	2D, SST $k-\omega$	Compared to other examined ORs, the elliptical profile's C_p improves at OR = 0.15.
Tahani M. et al. [105]	1	0	0 to 10 m/s [38]	0.1 to 1.1	2 (twisted conical)	SST	Compared to a wind rotor without a shaft and twist, the twisted wind rotor with a conical shaft performed better.
Tian W. et al. [106]	1.1	91 mm	7 m/s	0.6 to 1.2	2 (Optimised Semicircular)	2D, SST $k-\omega$	The the new rotor is 4.41 % more efficient than that of the traditional design.
Amiri M. et al. [107]	1	No overlap	7 m/s	0.2 to 0.8	2 (with valves)	3D, SST $k-\omega$	Compared to a traditional S-rotor, the turbine's maximum power coefficient has risen by 20.8 %.

Investigator(s)	AR	Overlap distance/OR	Wind velocity	TSR (λ) Operating range	No. of blades and cross section	CFD Methodology	Observation
Ebrahimpour, M. et al. [108]	-	0 to 0.2	6 to 9 m/s	0.2 to 1.4	2	2D, realizable K- ϵ	The optimal rotor has a horizontal overlap ratio of +0.15 and a vertical overlap ratio of -0.1.
Alom N. et al. [109]	0.91	15% of Chord i.e., 0.15d	6.2 m/s	0.6	2 (elliptical profile)	2D, SST k- ω	The drag coefficient of vented elliptical and semicircular-bladed rotors is higher than that of non-vented rotors.
Bai H. L. et al. [110]	-	15% of Chord i.e., 0.15d	4.05 m/s	0.2 to 1.5	2	2D, SST k- ω	Compared to open space, the power output of the S-rotor installed in the 2D channel can be increased by 200%.
Alom N. et al. [111]	-	-	5 m/s to 7 m/s	0.2 to 1.2	2 (elliptical, semi-circular, modified bach and benesh)	2D, SST k- ω	The elliptical profile has a peak C_p of 0.34 at TSR = 0.8, but the semicircular, Benesh, and modified Bach profiles have peak C_p s of 0.272, 0.294, and 0.304 at the same TSR.
Alom N. [112]	-	0.15	6.2 m/s	0.6	2	2D, SST k- ω	In the elliptical profile with curtain plates, the average coefficient of drag (C_{davg}) improves by 81.81 percent.
Mohammad Pourhosseinian et al. [113]	1.28	0.16 to 0.78	6 m/s	0.2 to 1.4	2	2D, RNG k- ϵ	The 2-D CFD results were compared to the 3-D model, and the predictions were good enough except at very low TSRs.
Al-Ghriybah et al. [114]	-	-	9 m/s	0.4 to 0.7	2 (each with 2 inner savonius blades)	2D, realizable k- ϵ	On a conventional S-rotor, the usefulness of the two inner blades has been demonstrated.
Salih Meri Al Absi et al. [115]	1	OR 0.1 to 0.2	9 m/s	0.2 to 1.4	2 (elliptical)	SST k- ω model	The elliptic zigzag surface blade savonius rotor outperforms the standard elliptic savonius rotor in terms of efficiency.
Ahmed S. Saad et al. [116]	1 to 4	0	6 m/s	0.2 to 1.4	2 (twisted blades)	3D, k- ω SST	Multi-stage rotors with twisted blades have a positive C_{ST} throughout the revolution, which improves the rotor's self-starting ability.

Investigator(s)	AR	Overlap distance/ OR	Wind velocity	TSR (λ) Operating range	No. of blades and cross section	CFD Methodology	Observation
M.H. Pranta et al. [117]	-	30 mm	12 m/s	0.5 to 1.2	2 (modified elliptical)	2D, SST k- ω	The optimum torque was 7.02 N-m, 62.5 % more than the standard design.

7 Summary and discussion on S-rotor:

TSR is a critical parameter for evaluating an S-rotor performance. This is because it directly impacts performance; researchers discovered that in most circumstances, a TSR of 0.7 to 1 is optimal. However, the S-rotor is recommended to be tested for TSR values ranging from 0.2 to 1.2.

In many investigations, an overlap ratio of 0.2 is said to improve the performance of the S-rotor. However, a few investigators noticed that as OR raised from 0.2 to 0.5, the performance of the S-rotor improved, then deteriorated. The S-rotor is recommended to be evaluated for ORs ranging from 0.2 to 0.5.

It needs to be noted that increasing the height or diameter of the S-rotor will aid tap more wind and hence improve performance. Therefore, when testing an S-rotor with a novel blade shape, it is recommended to evaluate the performance at aspect ratios ranging from 0.7 to 1.2.

It is observed that a two-bladed S-rotor performed better compared to three-bladed and four-bladed rotors. However, the starting characteristics were good for a three-bladed S-rotor.

Similarly, staging improves the starting characteristics, but as the number of stages increases the performance deteriorates. However, if testing a new blade shape or wind augmentation method, it is advised to vary and test the number of buckets and stages to know the optimal design.

The addition of endplates to the S-rotor improved its performance. The optimum endplate diameter is said to be $D_0=1.1D$. However, depending on the blade's novelty and the augmenting technique, the end plate design (dimensional specifications) can be changed to optimise the rotor's performance.

The performance of the S-rotor improves as the wind velocity increases. However, because S-rotor is more commonly used in built environments or low wind zones, most studies have evaluated it for low wind speeds ranging from 4 m/s to 9 m/s.

An S-rotor though is called a drag type VAWT, it still experiences a little of lift force. Therefore, it is a good practice to evaluate the S-rotors aerodynamic behaviour by finding the lift and drag coefficients at various angle of attacks of S-rotor, especially when testing a novel blade profiles and wind augmentation devices.

S-rotor experimental studies are usually carried out in a low-speed wind tunnel with the S-rotor in the test section or at the tunnel exit. To acquire accurate results, any blockage effects must be identified and rectified prior to the test. However, wind tunnel blockage effects are negligible when $BR < 10$. Nevertheless, a few wind tunnel blockage correction methods are used to tackle $BRs > 10$.

Furthermore, a BR around 39 % is reported to demonstrate minor blockage effect and may be ignored if the S-rotor is tested using an open jet wind tunnel or by placing at the exit side of the wind tunnel. However, there's no standard set length for testing an S-rotor at the exit of the wind tunnel.

According to a few researchers, an S-rotor must be kept at a distance of 2m away from the wind tunnel exit to maintain a uniform air stream.

Most studies' turbulent models revealed that the realizable model and RNG k- ϵ model are better than conventional k- ϵ and SA models. The standard k- ω turbulence model, on the other hand, predicts lower C_T and C_p values.

8 Conclusion and Recommendation:

Several experimental and computational studies have been undertaken over the last few decades to improve the efficiency of an S-rotor. This work attempts to compile test data from numerous previous studies to determine the test parameters that may be considered to evaluate the S-rotor's performance.

- Experimental test parameters used mainly by researchers are: TSR=0.2 to 1.2, AR=0.7 to 1.2, OR=0.2 to 0.5, $V=4$ m/s to 9 m/s, BR is to be considered as it affects the performance of S-rotor and eventually tests results. However, for $BR < 10$ blockage effect is negligible and need not be considered. Furthermore, it has been exposed that for BR of 39%, wind tunnel blockage effects for open jets can be ignored. In addition, to test the S-rotor with an open jet wind tunnel or at the wind tunnel exit section, a 2 m spacing between the S-rotor and the wind tunnel outlet is encouraged to be maintained for uniform airflow distribution.
 - More significant AR's are appropriate for S-rotors at higher wind speeds and vice versa.
 - Static torque increases with an increase in the blade overlap distance.
 - Elliptical bladed S-rotor proved to be efficient among all the blade profiles.
 - The number of buckets and stages impacts the S-rotor's aerodynamic behaviour.
 - C_T increases nearly linearly as TSR decreases.
- Computational test parameters used in most studies have shown that realizable and RNG k- ϵ models forecast better than regular k- ϵ and SA models. However, smaller C_T and C_P values are predicted by the classic k- ω model.

Several studies have demonstrated that blade profiles and wind augmentation techniques have a major impact on an S-rotor's efficiency, indicating room for improvement in blade profiles and wind augmentation methods.

Nomenclature

A	Swept area of S-rotor (m^2)
C_P	Power coefficient
C_T	Torque coefficient
C_{ST}	Static torque coefficient of S-rotor
d	Chord length of the S-rotor blade (m)
D	Diameter of S-rotor(m)
D_o	End plate diameter of the S-rotor (m)
C_D	Coefficient of drag force
C_L	Coefficient of lift force
e	Overlap distance between S-rotor blades (m)
H	S-rotor blade height (m)
k	Turbulence kinetic energy (m^2/s^2)
N	S-rotor rotational speed (rpm)
P_a	Power available in the wind (W)
P_t	Power produced by the S-rotor (W)
Re	Reynolds number
T_t	Turbine torque (Nm)
T_a	Torque available in the wind (Nm)
u	S-rotor tip speed (m/s)

v	Wind velocity (m/s)
R	Radius of S-rotor (m)

Symbols

α, β	Angle of attack (deg)
ρ	Density of air (kg/m ³)
ω	Angular velocity (rad/sec)

Abbreviations

TSR	Tip speed ratio
AR	Aspect ratio
BR	Blockage ratio
OR	Overlap ratio
CFD	Computational fluid dynamics
FEM	Finite element method
FVM	Finite volume method
FDM	Finite difference method
HAWT	Horizontal axis wind turbine
VAWT	Vertical axis wind turbine
RNG	Renormalized
SST	Shear stress transport

References:

- [1] S. Chu and A. Majumdar, "Opportunities and challenges for a sustainable energy future," *Nature*, vol. 488, no. 7411. pp. 294–303, 2012, doi: 10.1038/nature11475.
- [2] K. Marvel, B. Kravitz, and K. Caldeira, "Geophysical limits to global wind power," *Nat. Clim. Chang.*, vol. 3, no. 2, pp. 118–121, 2013, doi: 10.1038/nclimate1683.
- [3] E. Hau, *Wind turbines: Fundamentals, technologies, application, economics*. 2013.
- [4] J. T. Hansen, M. Mahak, and I. Tzanakis, "Numerical modelling and optimization of vertical axis wind turbine pairs: A scale up approach," *Renew. Energy*, vol. 171, pp. 1371–1381, 2021, doi: 10.1016/j.renene.2021.03.001.
- [5] M. M. Aslam Bhutta, N. Hayat, A. U. Farooq, Z. Ali, S. R. Jamil, and Z. Hussain, "Vertical axis wind turbine - A review of various configurations and design techniques," *Renewable and Sustainable Energy Reviews*, vol. 16, no. 4. pp. 1926–1939, 2012, doi: 10.1016/j.rser.2011.12.004.
- [6] F. Toja-Silva, A. Colmenar-Santos, and M. Castro-Gil, "Urban wind energy exploitation systems: Behaviour under multidirectional flow conditions - Opportunities and challenges," *Renewable and Sustainable Energy Reviews*, vol. 24. pp. 364–378, 2013, doi: 10.1016/j.rser.2013.03.052.
- [7] S. Eriksson, H. Bernhoff, and M. Leijon, "Evaluation of different turbine concepts for wind power," *Renewable and Sustainable Energy Reviews*, vol. 12, no. 5. pp. 1419–1434, 2008, doi: 10.1016/j.rser.2006.05.017.
- [8] J. V. Akwa, H. A. Vielmo, and A. P. Petry, "A review on the performance of Savonius wind turbines," *Renewable and Sustainable Energy Reviews*, vol. 16, no. 5. pp. 3054–3064, 2012, doi: 10.1016/j.rser.2012.02.056.
- [9] S. Roy and U. K. Saha, "Review on the numerical investigations into the design and development of Savonius wind rotors," *Renewable and Sustainable Energy Reviews*, vol. 24. pp. 73–83, 2013, doi:

10.1016/j.rser.2013.03.060.

- [10] X. Jin, G. Zhao, K. Gao, and W. Ju, "Darrieus vertical axis wind turbine: Basic research methods," *Renewable and Sustainable Energy Reviews*, vol. 42, pp. 212–225, 2015, doi: 10.1016/j.rser.2014.10.021.
- [11] D. G. Shepherd, "Historical Development of the Windmill," in *NASA Contractor Report 4337*, 1990.
- [12] P. D. Fleming and S. D. Probert, "The evolution of wind-turbines: An historical review," *Appl. Energy*, vol. 18, no. 3, pp. 163–177, 1984, doi: 10.1016/0306-2619(84)90007-2.
- [13] D. Kim and M. Gharib, "Efficiency improvement of straight-bladed vertical-axis wind turbines with an upstream deflector," *J. Wind Eng. Ind. Aerodyn.*, vol. 115, pp. 48–52, 2013, doi: 10.1016/j.jweia.2013.01.009.
- [14] D. A. Spera, "Wind Turbine Technology: Fundamental Concepts of Wind Turbine Engineering," *Sol. Energy*, 2009.
- [15] S. J. Savonius, "Rotor adapted to be driven by wind or flowing water," *Patent*, p. 8, 1929.
- [16] U. K. Saha, S. Thotla, and D. Maity, "Optimum design configuration of Savonius rotor through wind tunnel experiments," *J. Wind Eng. Ind. Aerodyn.*, vol. 96, no. 8–9, pp. 1359–1375, 2008, doi: 10.1016/j.jweia.2008.03.005.
- [17] M. A. Kamoji, S. B. Kedare, and S. V. Prabhu, "Experimental investigations on single stage, two stage and three stage conventional Savonius rotor," *Int. J. Energy Res.*, vol. 32, no. 10, pp. 877–895, 2008, doi: 10.1002/er.1399.
- [18] S. Frikha, Z. Driss, E. Ayadi, Z. Masmoudi, and M. S. Abid, "Numerical and experimental characterization of multi-stage Savonius rotors," *Energy*, vol. 114, pp. 382–404, 2016, doi: 10.1016/j.energy.2016.08.017.
- [19] S. Roy, P. Mukherjee, and U. K. Saha, "Aerodynamic performance evaluation of a novel savonius-style wind turbine under an oriented jet," 2014, doi: 10.1115/GTINDIA2014-8152.
- [20] K. H. Wong, W. T. Chong, N. L. Sukiman, S. C. Poh, Y. C. Shiah, and C. T. Wang, "Performance enhancements on vertical axis wind turbines using flow augmentation systems: A review," *Renewable and Sustainable Energy Reviews*, vol. 73, pp. 904–921, 2017, doi: 10.1016/j.rser.2017.01.160.
- [21] N. Alom and U. K. Saha, "Four Decades of Research into the Augmentation Techniques of Savonius Wind Turbine Rotor," *J. Energy Resour. Technol. Trans. ASME*, vol. 140, no. 5, 2018, doi: 10.1115/1.4038785.
- [22] S. J. Savonius, "Wind Rotor," *Patent*, p. 4, 1930.
- [23] M. Fernando, "On the performance and wake aerodynamics of the Savonius wind turbine," 1987.
- [24] M. H. Mohamed, G. Janiga, E. Pap, and D. Thévenin, "Optimal blade shape of a modified Savonius turbine using an obstacle shielding the returning blade," in *Energy Conversion and Management*, 2011, vol. 52, no. 1, pp. 236–242, doi: 10.1016/j.enconman.2010.06.070.
- [25] P. Quan and T. Leephakpreeda, "Assessment of wind energy potential for selecting wind turbines: An application to Thailand," *Sustain. Energy Technol. Assessments*, vol. 11, pp. 17–26, 2015, doi: 10.1016/j.seta.2015.05.002.
- [26] D. Le Gourrieres, "Wind power plants: theory and design.," 1982, doi: 10.1115/1.3267641.
- [27] B. D. Altan and M. Atilgan, "The use of a curtain design to increase the performance level of a Savonius wind rotors," *Renew. Energy*, vol. 35, no. 4, pp. 821–829, 2010, doi: 10.1016/j.renene.2009.08.025.
- [28] R. Carriveau, *Fundamental and Advanced Topics in Wind Power*. Intechopen, 2011.
- [29] N. Alom and U. K. Saha, "Evolution and progress in the development of savonius wind turbine rotor blade profiles and shapes," *Journal of Solar Energy Engineering, Transactions of the ASME*, vol. 141, no. 3, 2019, doi: 10.1115/1.4041848.
- [30] M. A. Kamoji, S. B. Kedare, and S. V. Prabhu, "Experimental investigations on the effect of overlap

ratio and blade edge conditions on the performance of conventional Savonius rotor,” *Wind Eng.*, vol. 32, no. 2, pp. 163–178, 2008, doi: 10.1260/030952408784815826.

- [31] K. Sobczak, “Numerical investigations of an influence of the aspect ratio on the Savonius rotor performance,” in *Journal of Physics: Conference Series*, 2018, vol. 1101, no. 1, doi: 10.1088/1742-6596/1101/1/012034.
- [32] S. Roy and U. K. Saha, “Investigations on the effect of aspect ratio into the performance of savonius rotors,” 2013, doi: 10.1115/GTINDIA2013-3729.
- [33] G. Bach, “Untersuchungen über Savonius-Rotoren und verwandte Strömungsmaschinen,” *Forsch. auf dem Gebiete des Ingenieurwesens*, vol. 2, no. 6, pp. 218–231, 1931, doi: 10.1007/BF02579117.
- [34] I. Ushiyama, H. Nagai, and J. Shinoda, “Experimentally Determining the Optimum Design Configuration for Savonius Rotors,” *Trans. Japan Soc. Mech. Eng. Ser. B*, vol. 52, no. 480, pp. 2973–2982, 1986, doi: 10.1299/kikaib.52.2973.
- [35] M. A. Kamoji, S. B. Kedare, and S. V. Prabhu, “Performance tests on helical Savonius rotors,” *Renew. Energy*, vol. 34, no. 3, pp. 521–529, 2009, doi: 10.1016/j.renene.2008.06.002.
- [36] T. Zhou and D. Rempfer, “Numerical study of detailed flow field and performance of Savonius wind turbines,” *Renew. Energy*, vol. 51, pp. 373–381, 2013, doi: 10.1016/j.renene.2012.09.046.
- [37] K. Kacprzak, G. Liskiewicz, and K. Sobczak, “Numerical investigation of conventional and modified Savonius wind turbines,” *Renew. Energy*, vol. 60, pp. 578–585, 2013, doi: 10.1016/j.renene.2013.06.009.
- [38] S. Roy and U. K. Saha, “Wind tunnel experiments of a newly developed two-bladed Savonius-style wind turbine,” *Appl. Energy*, vol. 137, pp. 117–125, 2015, doi: 10.1016/j.apenergy.2014.10.022.
- [39] N. Alom, B. Borah, and U. K. Saha, “An insight into the drag and lift characteristics of modified Bach and Benesh profiles of Savonius rotor,” in *Energy Procedia*, 2018, vol. 144, pp. 50–56, doi: 10.1016/j.egypro.2018.06.007.
- [40] A. E. Saad El-Deen, M. A. A. Nawar, Y. A. Attai, and R. M. Abd El-Maksoud, “On the enhancement of Savonius Bach-type rotor performance by studying the optimum stator configuration,” *Ocean Eng.*, vol. 217, 2020, doi: 10.1016/j.oceaneng.2020.107954.
- [41] T. K. Aldos, “SAVONIUS ROTOR USING SWINGING BLADES AS AN AUGMENTATION SYSTEM.,” *Wind Eng.*, 1984.
- [42] A. H. Benesh, “Wind turbine system using a vertical axis savonius-type rotor,” *Google Patents / US Pat. 4,784,568*, 1988.
- [43] A. H. Benesh, “Benesh wind turbine,” 1992.
- [44] P. Reupke and S. D. Probert, “Slatted-blade Savonius wind-rotors,” *Appl. Energy*, vol. 40, no. 1, pp. 65–75, 1991, doi: 10.1016/0306-2619(91)90051-X.
- [45] J. H. Lee, Y. T. Lee, and H. C. Lim, “Effect of twist angle on the performance of Savonius wind turbine,” *Renew. Energy*, vol. 89, pp. 231–244, 2016, doi: 10.1016/j.renene.2015.12.012.
- [46] A. S. Saad, I. I. El-Sharkawy, S. Ookawara, and M. Ahmed, “Performance enhancement of twisted-bladed Savonius vertical axis wind turbines,” *Energy Convers. Manag.*, vol. 209, 2020, doi: 10.1016/j.enconman.2020.112673.
- [47] S. Hadi, M. Sidiq, D. C. Anindito, A. Prasetyo, D. D. D. P. Tjahjana, and R. Hadiani, “Experimental study of the effects of blade twist on the performance of Savonius water turbine in water pipe,” *J. Adv. Res. Fluid Mech. Therm. Sci.*, vol. 57, no. 2, pp. 202–207, 2019.
- [48] A. Zakaria and M. S. N. Ibrahim, “Effect of twist angle on starting capability of a Savonius rotor - CFD analysis,” in *IOP Conference Series: Materials Science and Engineering*, 2020, vol. 715, no. 1, doi: 10.1088/1757-899X/715/1/012014.
- [49] A. Damak, Z. Driss, and M. S. Abid, “Experimental investigation of helical Savonius rotor with a twist of 180°,” *Renew. Energy*, vol. 52, pp. 136–142, 2013, doi: 10.1016/j.renene.2012.10.043.

- [50] A. S. Grinspan, U. K. Saha, and P. Mahanta, "Experimental investigation of twisted bladed savonius wind turbine rotor," *Int. Energy J.*, vol. 5, no. 1, pp. 1–9, 2004.
- [51] L. Song, Z. X. Yang, R. T. Deng, and X. G. Yang, "Performance and structure optimization for a new type of vertical axis wind turbine," in *International Conference on Advanced Mechatronic Systems, ICAMechS*, 2013, pp. 687–692, doi: 10.1109/ICAMechS.2013.6681730.
- [52] A. Alaimo, A. Milazzo, F. Trentacosti, and A. Esposito, "On the effect of slotted blades on Savonius wind generator performances by CFD analysis," in *Advanced Materials Research*, 2012, vol. 512–515, pp. 747–753, doi: 10.4028/www.scientific.net/AMR.512-515.747.
- [53] A. Alaimo, A. Esposito, A. Milazzo, C. Orlando, and F. Trentacosti, "Slotted blades savonius wind turbine analysis by CFD," *Energies*, vol. 6, no. 12, pp. 6335–6351, 2013, doi: 10.3390/en6126335.
- [54] F. Wenehenubun, A. Saputra, and H. Sutanto, "An experimental study on the performance of Savonius wind turbines related with the number of blades," in *Energy Procedia*, 2015, vol. 68, pp. 297–304, doi: 10.1016/j.egypro.2015.03.259.
- [55] N. H. Mahmoud, A. A. El-Haroun, E. Wahba, and M. H. Nasef, "An experimental study on improvement of Savonius rotor performance," *Alexandria Eng. J.*, vol. 51, no. 1, pp. 19–25, 2012, doi: 10.1016/j.aej.2012.07.003.
- [56] M. D. Huda, M. A. Selim, A. K. M. S. Islam, and M. Q. Islam, "Performance of an S-shaped savonius rotor with a deflecting plate," *RERIC Int. Energy J.*, 1992.
- [57] V. J. Modi and M. S. U. K. Fernando, "Unsteady aerodynamics and wake of the savonius wind turbine: A numerical study," *J. Wind Eng. Ind. Aerodyn.*, vol. 46–47, no. C, pp. 811–816, 1993, doi: 10.1016/0167-6105(93)90357-T.
- [58] P. Jaohindy, S. McTavish, F. Garde, and A. Bastide, "An analysis of the transient forces acting on Savonius rotors with different aspect ratios," *Renew. Energy*, vol. 55, pp. 286–295, 2013, doi: 10.1016/j.renene.2012.12.045.
- [59] K. Irabu and J. N. Roy, "Study of direct force measurement and characteristics on blades of Savonius rotor at static state," *Exp. Therm. Fluid Sci.*, vol. 35, no. 4, pp. 653–659, 2011, doi: 10.1016/j.expthermflusci.2010.12.015.
- [60] S. Roy and U. K. Saha, "An adapted blockage factor correlation approach in wind tunnel experiments of a Savonius-style wind turbine," *Energy Convers. Manag.*, vol. 86, pp. 418–427, 2014, doi: 10.1016/j.enconman.2014.05.039.
- [61] A. J. Alexander and B. P. Holownia, "Wind tunnel tests on a savonius rotor," *J. Wind Eng. Ind. Aerodyn.*, vol. 3, no. 4, pp. 343–351, 1978, doi: 10.1016/0167-6105(78)90037-5.
- [62] T. Ogawa and H. Yoshida, "The effects of a deflecting plate and rotor end plates on performances of Savonius-type wind turbine.," *Bull. Jsme*, vol. 46, no. 5, Oct. 1985, pp. 2115–2121, 1985, doi: 10.1299/jsme1958.29.2115.
- [63] B. M. Shaughnessy and S. D. Probert, "Partially-blocked savonius rotor," *Appl. Energy*, vol. 43, no. 4, pp. 239–249, 1992, doi: 10.1016/0306-2619(92)90024-6.
- [64] M. J. Rajkumar and U. K. Saha, "Valve-aided twisted Savonius rotor," *Wind Eng.*, vol. 30, no. 3, pp. 243–254, 2006, doi: 10.1260/030952406778606269.
- [65] B. D. Altan and M. Atilgan, "An experimental and numerical study on the improvement of the performance of Savonius wind rotor," *Energy Convers. Manag.*, vol. 49, no. 12, pp. 3425–3432, 2008, doi: 10.1016/j.enconman.2008.08.021.
- [66] B. Plourde, J. Abraham, G. Mowry, and W. Minkowycz, "An experimental investigation of a large, vertical-axis wind turbine: Effects of venting and capping," *Wind Eng.*, vol. 35, no. 2, pp. 213–222, 2011, doi: 10.1260/0309-524X.35.2.213.
- [67] W. Yahya, K. Ziming, W. Juan, M. S. Qurashi, M. Al-Nehari, and E. Salim, "Influence of tilt angle and the number of guide vane blades towards the Savonius rotor performance," *Energy Reports*, vol. 7, pp. 3317–3327, 2021, doi: 10.1016/j.egypro.2021.05.053.

- [68] A. Grönman, J. Tiainen, and A. Jaatinen-Värri, “Experimental and analytical analysis of vaned savonius turbine performance under different operating conditions,” *Appl. Energy*, vol. 250, pp. 864–872, 2019, doi: 10.1016/j.apenergy.2019.05.105.
- [69] M. Tartuferi, V. D’Alessandro, S. Montelpare, and R. Ricci, “Enhancement of savonius wind rotor aerodynamic performance: A computational study of new blade shapes and curtain systems,” *Energy*, 2015, doi: 10.1016/j.energy.2014.11.023.
- [70] S. Tourn, J. Pallarès, I. Cuesta, and U. S. Paulsen, “Characterization of a new open jet wind tunnel to optimize and test vertical axis wind turbines,” *J. Renew. Sustain. Energy*, vol. 9, no. 3, 2017, doi: 10.1063/1.4982750.
- [71] V. J. Modi and M. S. U. K. Fernando, “On the performance of the savonius wind turbine,” *J. Sol. Energy Eng. Trans. ASME*, vol. 111, no. 1, pp. 71–81, 1989, doi: 10.1115/1.3268289.
- [72] N. Fujisawa and F. Gotoh, “Experimental study on the aerodynamic performance of a savonius rotor,” *J. Sol. Energy Eng. Trans. ASME*, vol. 116, no. 3, pp. 148–152, 1994, doi: 10.1115/1.2930074.
- [73] M. H. Nasef, W. A. El-Askary, A. A. AbdEL-hamid, and H. E. Gad, “Evaluation of Savonius rotor performance: Static and dynamic studies,” *J. Wind Eng. Ind. Aerodyn.*, vol. 123, pp. 1–11, 2013, doi: 10.1016/j.jweia.2013.09.009.
- [74] A. Banerjee, S. Roy, P. Mukherjee, and U. K. Saha, “Unsteady flow analysis around an elliptic-bladed savonius-style wind turbine,” 2014, doi: 10.1115/GTINDIA2014-8141.
- [75] K. S. Jeon, J. I. Jeong, J. K. Pan, and K. W. Ryu, “Effects of end plates with various shapes and sizes on helical Savonius wind turbines,” *Renew. Energy*, vol. 79, no. 1, pp. 167–176, 2015, doi: 10.1016/j.renene.2014.11.035.
- [76] R. Ricci, R. Romagnoli, S. Montelpare, and D. Vitali, “Experimental study on a Savonius wind rotor for street lighting systems,” *Applied Energy*, vol. 161, pp. 143–152, 2016, doi: 10.1016/j.apenergy.2015.10.012.
- [77] O. O. Mojola, “On the aerodynamic design of the savonius windmill rotor,” *J. Wind Eng. Ind. Aerodyn.*, vol. 21, no. 2, pp. 223–231, 1985, doi: 10.1016/0167-6105(85)90005-4.
- [78] J. Chen, K. Jan, L. Zhang, L. Lu, and H. Yang, “Influence of phase-shift and overlap ratio on savonius wind turbine’s performance,” *J. Sol. Energy Eng. Trans. ASME*, vol. 134, no. 1, 2012, doi: 10.1115/1.4004980.
- [79] J. Kumbennuss, J. Chen, H. X. Yang, and L. Lu, “Investigation into the relationship of the overlap ratio and shift angle of double stage three bladed vertical axis wind turbine (VAWT),” *J. Wind Eng. Ind. Aerodyn.*, vol. 107–108, pp. 57–75, 2012, doi: 10.1016/j.jweia.2012.03.021.
- [80] V. J. Modi, N. J. Roth, and A. Pittalwala, “Blade configurations and performance of the savonius rotor with application to an irrigation system in Indonesia,” *J. Sol. Energy Eng. Trans. ASME*, vol. 105, no. 3, pp. 294–299, 1983, doi: 10.1115/1.3266381.
- [81] T. Hayashi, Y. Li, and Y. Hara, “Wind tunnel tests on a different phase three-stage Savonius rotor,” *JSME Int. Journal, Ser. B Fluids Therm. Eng.*, vol. 48, no. 1, pp. 9–16, 2005, doi: 10.1299/jsmeb.48.9.
- [82] A. Damak, Z. Driss, and M. S. Abid, “Optimization of the helical Savonius rotor through wind tunnel experiments,” *J. Wind Eng. Ind. Aerodyn.*, vol. 174, pp. 80–93, 2018, doi: 10.1016/j.jweia.2017.12.022.
- [83] P. R. Spalart, S. R. Allmaras, and J. Reno, “One-Equation Turbulence Model for Aerodynamic Flows,” *30th Aerosp. Sci. Meet. Exhib.*, p. 23, 1992.
- [84] C. Song, Y. Zheng, Z. Zhao, Y. Zhang, C. Li, and H. Jiang, “Investigation of meshing strategies and turbulence models of computational fluid dynamics simulations of vertical axis wind turbines,” *J. Renew. Sustain. Energy*, vol. 7, no. 3, 2015, doi: 10.1063/1.4921578.
- [85] Y. Hu, Z. Tong, and S. Wang, “A new type of VAWT and blade optimization,” in *IET Conference Publications*, 2009, vol. 2009, no. 556 CP, doi: 10.1049/cp.2009.1392.
- [86] B. Emmanuel and W. Jun, “Numerical study of a six-bladed savonius wind turbine,” *J. Sol. Energy Eng. Trans. ASME*, vol. 133, no. 4, 2011, doi: 10.1115/1.4004549.

- [87] R. Howell, N. Qin, J. Edwards, and N. Durrani, "Wind tunnel and numerical study of a small vertical axis wind turbine," *Renew. Energy*, vol. 35, no. 2, pp. 412–422, 2010, doi: 10.1016/j.renene.2009.07.025.
- [88] J. P. Abraham, B. D. Plourde, G. S. Mowry, W. J. Minkowycz, and E. M. Sparrow, "Summary of Savonius wind turbine development and future applications for small-scale power generation," *Journal of Renewable and Sustainable Energy*, vol. 4, no. 4, 2012, doi: 10.1063/1.4747822.
- [89] Z. Zhao, Y. Zheng, X. Xu, W. Liu, and G. Hu, "Research on the improvement of the performance of savonius rotor based on numerical study," 2009, doi: 10.1109/SUPERGEN.2009.5348197.
- [90] A. Kianifar and M. Anbarsooz, "Blade curve influences on the performance of Savonius rotors: Experimental and numerical," in *Proceedings of the Institution of Mechanical Engineers, Part A: Journal of Power and Energy*, 2011, vol. 225, no. 3, pp. 343–350, doi: 10.1177/2041296710394413.
- [91] B. Plourde, J. Abraham, G. Mowry, and W. Minkowycz, "Simulations of three-dimensional vertical-axis turbines for communications applications," *Wind Eng.*, vol. 36, no. 4, pp. 443–454, 2012, doi: 10.1260/0309-524X.36.4.443.
- [92] S. Roy and U. K. Saha, "Computational study to assess the influence of overlap ratio on static torque characteristics of a vertical axis wind turbine," in *Procedia Engineering*, 2013, vol. 51, pp. 694–702, doi: 10.1016/j.proeng.2013.01.099.
- [93] P. Jaohindy, H. Ennamiri, F. Garde, and A. Bastide, "Numerical investigation of airflow through a Savonius rotor," *Wind Energy*, vol. 17, no. 6, pp. 853–868, 2014, doi: 10.1002/we.1601.
- [94] K. Kacprzak and K. Sobczak, "Computational assessment of the influence of the overlap ratio on the power characteristics of a Classical Savonius wind turbine," *Open Eng.*, vol. 5, no. 1, pp. 314–322, 2015, doi: 10.1515/eng-2015-0039.
- [95] A. M. Baz, N. A. Mahmoud, A. M. Hamed, and K. M. Youssef, "Optimization of two and three rotor savonius wind turbine," in *Proceedings of the ASME Turbo Expo*, 2015, vol. 9, doi: 10.1115/GT2015-43988.
- [96] Z. Mao and W. Tian, "Effect of the blade arc angle on the performance of a Savonius wind turbine," *Adv. Mech. Eng.*, vol. 7, no. 5, pp. 1–10, 2015, doi: 10.1177/1687814015584247.
- [97] Z. Driss, O. Mlayeh, S. Driss, D. Driss, M. Maaloul, and M. S. Abid, "Study of the bucket design effect on the turbulent flow around unconventional Savonius wind rotors," *Energy*, vol. 89, pp. 708–729, 2015, doi: 10.1016/j.energy.2015.06.023.
- [98] W. Tian, B. Song, J. H. Van Zwieten, and P. Pyakurel, "Computational fluid dynamics prediction of a modified savonius wind turbine with novel blade shapes," *Energies*, vol. 8, no. 8, pp. 7915–7929, 2015, doi: 10.3390/en8087915.
- [99] M. Shaheen, M. El-Sayed, and S. Abdallah, "Numerical study of two-bucket Savonius wind turbine cluster," *J. Wind Eng. Ind. Aerodyn.*, vol. 137, pp. 78–89, 2015, doi: 10.1016/j.jweia.2014.12.002.
- [100] W. A. El-Askary, M. H. Nasef, A. A. AbdEL-hamid, and H. E. Gad, "Harvesting wind energy for improving performance of savonius rotor," *J. Wind Eng. Ind. Aerodyn.*, vol. 139, pp. 8–15, 2015, doi: 10.1016/j.jweia.2015.01.003.
- [101] Z. Driss, O. Mlayeh, S. Driss, M. Maaloul, and M. S. Abid, "Study of the incidence angle effect on the aerodynamic structure characteristics of an incurved Savonius wind rotor placed in a wind tunnel," *Energy*, vol. 113, pp. 894–908, 2016, doi: 10.1016/j.energy.2016.07.112.
- [102] N. Alom, S. C. Kolaparthi, S. C. Gadde, and U. K. Saha, "Aerodynamic design optimization of elliptical-bladed savonius-style wind turbine by numerical simulations," in *Proceedings of the International Conference on Offshore Mechanics and Arctic Engineering - OMAE*, 2016, vol. 6, doi: 10.1115/OMAEE2016-55095.
- [103] H. Moazam Sheikh, Z. Shabbir, H. Ahmed, M. H. Waseem, and M. Z. Sheikh, "Computational fluid dynamics analysis of a modified Savonius rotor and optimization using response surface methodology," *Wind Eng.*, vol. 41, no. 5, pp. 285–296, 2017, doi: 10.1177/0309524X17709732.

- [104] N. Alom and U. K. Saha, "Arriving at the optimum overlap ratio for an elliptical-bladed savonius rotor," in *Proceedings of the ASME Turbo Expo*, 2017, vol. 9, doi: 10.1115/GT2017-64137.
- [105] M. Tahani, A. Rabbani, A. Kasaeian, M. Mehrpooya, and M. Mirhosseini, "Design and numerical investigation of Savonius wind turbine with discharge flow directing capability," *Energy*, vol. 130, pp. 327–338, 2017, doi: 10.1016/j.energy.2017.04.125.
- [106] W. Tian, Z. Mao, B. Zhang, and Y. Li, "Shape optimization of a Savonius wind rotor with different convex and concave sides," *Renew. Energy*, 2018, doi: 10.1016/j.renene.2017.10.067.
- [107] M. Amiri and M. Anbarsooz, "Improving the Energy Conversion Efficiency of a Savonius Rotor Using Automatic Valves," *J. Sol. Energy Eng. Trans. ASME*, vol. 141, no. 3, 2019, doi: 10.1115/1.4042828.
- [108] M. Ebrahimpour, R. Shafaghat, R. Alamian, and M. S. Shadloo, "Numerical investigation of the Savonius vertical axis wind turbine and evaluation of the effect of the overlap parameter in both horizontal and vertical directions on its performance," *Symmetry (Basel)*, vol. 11, no. 6, 2019, doi: 10.3390/sym11060821.
- [109] N. Alom and U. K. Saha, "Drag and lift characteristics of a novel elliptical-bladed savonius rotor with vent augmenters," *J. Sol. Energy Eng. Trans. ASME*, vol. 141, no. 5, 2019, doi: 10.1115/1.4043516.
- [110] H. L. Bai, C. M. Chan, X. M. Zhu, and K. M. Li, "A numerical study on the performance of a Savonius-type vertical-axis wind turbine in a confined long channel," *Renew. Energy*, vol. 139, pp. 102–109, 2019, doi: 10.1016/j.renene.2019.02.044.
- [111] N. Alom and U. K. Saha, "Influence of blade profiles on Savonius rotor performance: Numerical simulation and experimental validation," *Energy Convers. Manag.*, vol. 186, pp. 267–277, 2019, doi: 10.1016/j.enconman.2019.02.058.
- [112] N. Alom, "Influence of curtain plates on the aerodynamic performance of an elliptical bladed Savonius rotor (S-rotor)," *Energy Syst.*, vol. 13, no. 1, pp. 265–280, 2021, doi: 10.1007/s12667-021-00428-w.
- [113] M. Pourhoseinian, S. Sharifian, and N. Asasian-Kolur, "Unsteady-state numerical analysis of advanced Savonius wind turbine," *Energy Sources, Part A Recover. Util. Environ. Eff.*, 2021, doi: 10.1080/15567036.2020.1859011.
- [114] M. Al-Ghriyah, M. Fadhli Zulkafli, D. Hissein Didane, and S. Mohd, "The effect of spacing between inner blades on the performance of the Savonius wind turbine," *Sustain. Energy Technol. Assessments*, vol. 43, 2021, doi: 10.1016/j.seta.2020.100988.
- [115] S. Meri Al Absi, A. Hasan Jabbar, S. Oudah Mezan, B. Ahmed Al-Rawi, and S. Thajeel Alattabi, "An experimental test of the performance enhancement of a Savonius turbine by modifying the inner surface of a blade," in *Materials Today: Proceedings*, 2021, vol. 42, pp. 2233–2240, doi: 10.1016/j.matpr.2020.12.309.
- [116] A. S. Saad, A. Elwardany, I. I. El-Sharkawy, S. Ookawara, and M. Ahmed, "Performance evaluation of a novel vertical axis wind turbine using twisted blades in multi-stage Savonius rotors," *Energy Convers. Manag.*, vol. 235, 2021, doi: 10.1016/j.enconman.2021.114013.
- [117] M. H. Pranta, M. S. Rabbi, and M. M. Roshid, "A computational study on the aerodynamic performance of modified savonius wind turbine," *Results Eng.*, vol. 10, 2021, doi: 10.1016/j.rineng.2021.100237.